Current Science
CS 5 (5), 4850-4862 (2025)
Received 18 July 2025 | **Revised 19 August** 2025 | **Accepted 15 September** 2025 | **Online Available 15 October** 2025
https://doi.org0/10.52845/CS/2025-5-5-38

Current Science

Current Science

OPEN ACCESS

ISSN(O)2795-8639

Research Article

An Improved Current Differential Protection in the MMC-based DC Distribution Network

Wei Jin[1], Shiguang Feng[2], Xiaoye Wu[1]

[1]College of New Energy, Jiangsu Vocational Institute of Architectural Technology, Xuzhou, China

[2]State Grid Lianyungang Power Supply Company, Lianyungang, China

[*]Corresponding Author: Wei Jin

Abstract:
When a fault occurs on an AC line connected to a Modular Multilevel Converter (MMC) station in a flexible DC distribution network, the short-circuit current on the MMC side is influenced by its control strategy—such as phase angle control and current limiting—resulting in characteristics significantly different from those in traditional distribution networks. Consequently, conventional current differential protection (CDP) may exhibit insufficient sensitivity or even fail to operate. First, based on the symmetrical component method, this paper analyzes the substantial difference in fault current magnitude between the MMC side and the grid side. Furthermore, the impact of the MMC station on the performance of CDP is specifically discussed under high transition resistance conditions. Given the current-limiting behavior and the theoretically infinite negative-sequence impedance on the MMC side, a novel current amplitude differential protection scheme is proposed. This method utilizes the current amplitudes from both ends, reducing the requirement for synchronized sampling and making it particularly suitable for distribution networks with limited communication capabilities. Finally, a simulation model is developed in MATLAB, and the results validate the effectiveness of the proposed approach.

Keywords: flexible DC distribution network, tie line fault, negative sequence current, current differential protection

I. Introduction

In pursuit of carbon peaking and neutrality goals, sustainable energy applications are being increasingly emphasized. The share of renewable sources such as wind and solar power continues to rise, along with an increasing proportion of DC loads in distribution networks. These evolving source-load characteristics necessitate more flexible grid access methods [1-2]. Against this backdrop, the flexible DC distribution network based on the Modular Multilevel Converter (MMC) has developed rapidly owing to its high controllability and interoperability, facilitating a transition from AC to AC-DC hybrid distribution systems [3-4].

The AC side of hybrid systems retains the technical advantages of conventional distribution networks, while the DC side offers superior power quality, extended power supply range, higher capacity, and more convenient integration of distributed generation [5-8]. In recent years, numerous hybrid AC-DC distribution demonstration projects have been implemented [9], confirming this architecture as a major development direction for future power systems [10].

Reliable protection is crucial for secure and stable system operation. In hybrid AC-DC systems, the fault current contributed by the MMC station is highly dependent on its control strategy. As a result, conventional current differential protection (CDP), designed based on traditional AC fault characteristics, often performs inadequately

[11,12]. Analyzing the impact of flexible DC systems on CDP and developing corresponding improved protection strategies are therefore essential to ensure system security—a topic that has attracted significant research attention.

Studies such as [13] and [14] examine the short-circuit current characteristics of MMC systems under various control strategies and propose computational methods, providing a theoretical basis for fault analysis. Liang Y. and Shi B. [15,16] identify key factors that impair CDP reliability, including fault type, power command values, and transition resistance. While these studies clarify why conventional CDP is unsuitable for hybrid systems, they do not offer specific solutions.

To mitigate the adverse impact of flexible DC systems on CDP, reference [17] enhances protection adaptability by coordinating the activation of MMC-side and AC-side protections. However, this approach overlooks the reactive power support capability of MMC stations during faults and underutilizes their fault characteristics. Li B. [18] proposes a scheme using the phase angle difference between line-end currents to design an adaptive braking coefficient, reducing the braking effect during internal faults. Liang Y. [19] introduces correction factors based on differences in current amplitude and phase between the two ends of the line during internal and external faults, improving CDP sensitivity and reliability by adjusting the braking and differential currents. Nevertheless, the method in [18] offers limited adjustment range and may still fail to operate when the operating and braking currents differ significantly. The approach in [19] is sensitive to current amplitude ratios but may be unreliable when amplitudes are similar.

Inverter-interfaced renewable power plants and MMC stations share certain fault characteristics. Improved CDP schemes for AC lines connected to such renewable plants are proposed in [20-22], and studies [23-25] investigate sequence components under inverter control strategies during faults, using positive-, negative-, and zero-sequence currents as auxiliary criteria to enhance the sensitivity and accuracy of protection. However, these methods may not be directly applicable to lines connected to MMC stations, which can operate in both rectifying and inverting modes. This operational flexibility may lead to maloperation under certain conditions.

Overall, current research focuses mainly on the adaptation and improvement of differential protection in MMC-HVDC systems, with limited attention paid to flexible DC distribution networks. Unlike MMC-HVDC systems, the operating state of an MMC station in a distribution network varies with source-load conditions and may frequently switch between rectifier and inverter modes. Moreover, communication infrastructure in distribution networks is often weaker than in transmission systems. Therefore, there is an urgent need for protection schemes tailored to the actual conditions of distribution networks.

This paper first analyzes the fault current characteristics of AC-side tie lines connected to MMC stations based on their control strategies. Using this analysis, the limitations of conventional CDP are evaluated. A new current amplitude differential protection scheme is proposed, which fully utilizes the limited fault current and high negative-sequence impedance characteristics of the MMC side. This scheme reduces the requirement for synchronous sampling and is better suited to the communication conditions of distribution networks. Simulation results validate the correctness of the theoretical analysis and demonstrate the superiority of the proposed protection method.

II. Analysis of Fault Currents

The typical structure of a flexible DC distribution network is illustrated in Fig. 1, based on the demonstration project [26].

A. MMC Side Fault Current Characteristic

When a fault occurs on the tie line, the short-circuit current depends on the control strategy of the MMC station and the wiring configuration of the transformer. The MMC station is only influenced by positive and negative sequence components passing through the transformer.

Negative sequence voltage can induce an undesirable negative sequence current in the MMC station, potentially causing the fault current to exceed the current capacity of the power electronic devices. To ensure equipment safety during faults, the MMC control strategy is

designed to suppress negative sequence current and limit positive sequence current.

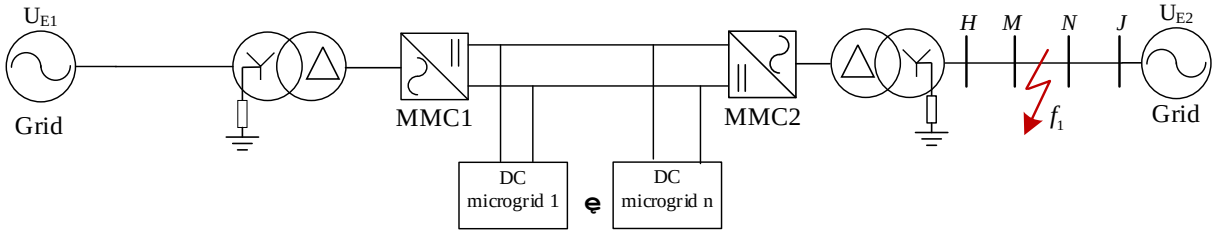

Figure1 The topology of a two-terminal flexible DC distribution network.

The control system responds within milliseconds after a fault occurs. Thus, the short-circuit current supplied by the MMC station is effectively determined by the outer-loop power controller. To prevent exceeding the current limits of the power devices, the output of the outer-loop power controller is clamped. Under non-severe fault conditions, the positive sequence current typically does not reach the saturation limit. The output current of the MMC is influenced by the power setpoint and the positive sequence voltage at the point of common coupling.

In summary, the control strategy of the MMC suppresses negative-sequence current and limits the amplitude of the positive-sequence current during faults. Due to cost considerations, power devices are typically designed with small current margins in practice, with saturation limits usually set between 1.1-1.2 p.u. Thus, the MMC station can be approximated as a controlled positive-sequence current source, with an amplitude close to the normal operating value.

B. The Line Side Fault Current Characteristics

The transformer blocks the zero-sequence current path between the converter and the AC line. Therefore, the magnitude of the zero-sequence current depends solely on the fault type, rather than the MMC station. When a fault occurs on the tie line, the fault current on the MMC side consists of an uncontrolled zero-sequence current, a controlled positive-sequence current, and a controlled negative-sequence current. Based on whether zero-sequence current is generated, faults can be categorized into grounded and ungrounded types.

Taking a single-line-to-ground fault (phase A) as an example, the fault current characteristics at both ends of the line are analyzed as follows. The schematic diagrams of the sequence component networks are shown in Fig. 2. Z_T is the transformer leakage reactance. Z_L is the impedance of the line MN. R_f is the transition resistance at the fault location. $\boldsymbol{\alpha}$ is the ratio of the distance from bus M to the fault point to the length of line MN. $\dot{U}^{-}_{mmc}$ represents the equivalent negative sequence voltage of the MMC.

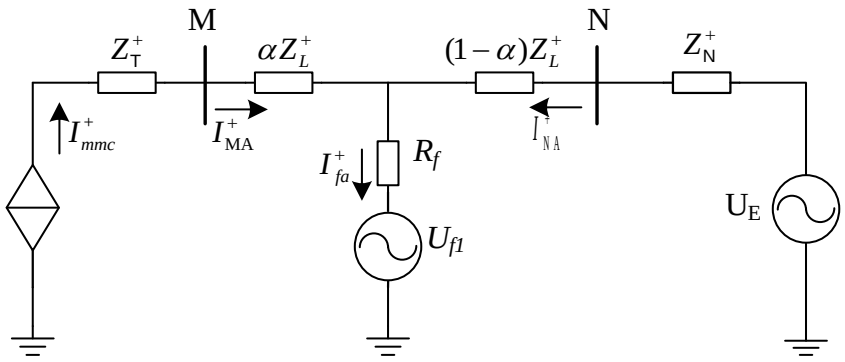

(a) Positive sequence network

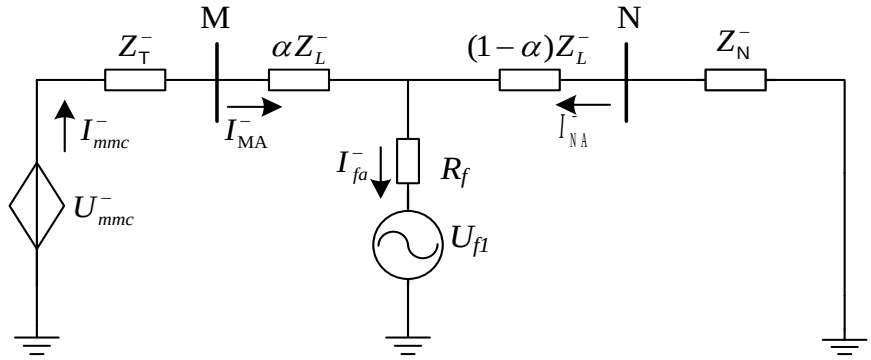

(b) Negative sequence \ network

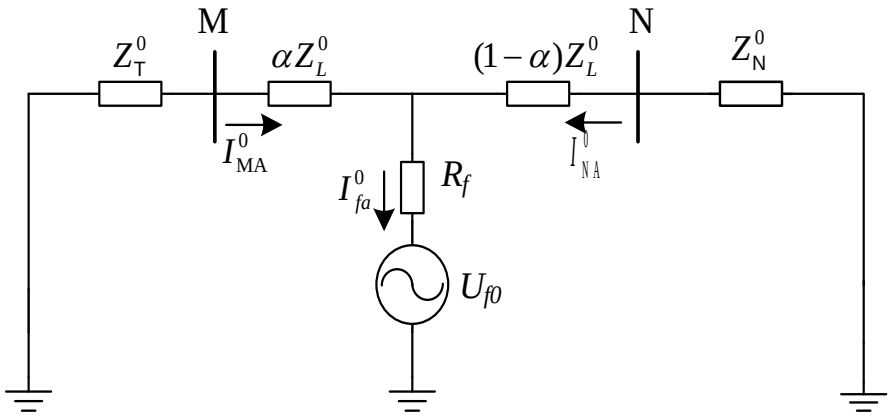

(c) Zero sequence network

Figure 2 Sequence component networks.

The fault current on the MMC side ($\boldsymbol{I}_{\mathbf{MA}}$) can be written as:

$$\begin{cases} \dot{I}_{MA} = \dot{I}_{MA} + \dot{I}_{MA} + \dot{I}_{MA} \\ \dot{I}_{MA} = I_{mmc}\angle(\theta+\delta) \\ \theta = \arctan(-Q_S / P_S) = \arctan(i_{vq}^{+*}/i_{vd}^{+*}) \end{cases} \quad (1)$$

Where $\boldsymbol{\theta}$ represents the phase difference between the A-phase current and voltage on the M side, and its magnitude is determined by the operating state of the MMC station that the actual active power and reactive power (P*s*, Q*s*) are output by the MMC station. When faults occur in the tie line, Q*s* is usually a positive value to provide voltage support for the power system. While the magnitude of P*s* depends on the operating state of the MMC station. To maintain power balance in the distribution network, P*s* can be either positive or negative. Therefore, $\boldsymbol{\theta} \subseteq(-\pi, 0)$. $\boldsymbol{\delta}$ is the voltage phase difference between the M side and the N side, which is smaller in practice and is not considered.

The sequence currents flowing into fault location f_1 are equal, which can be written as:

$$\dot{I}_{fa} = \dot{I}_{fa} = \dot{I}_{fa} = \frac{\dot{U}_{f1|0|}}{Z_{S1} + Z_{S2} + Z_{S0} + 3R_f} \quad (2)$$

Where Z_{S1}, Z_{S2}, and Z_{S0} represent trepresent the equivalent positive-, negative-, and zero-sequence impedances of the AC system, respectively, and denotes the pre-fault phase-A voltage under normal operating conditions. As illustrated in Fig.2(c), the zero-sequence current is generated by

the combined action of the zero-sequence voltage at the fault point and the system's zero-sequence impedance. Since the zero-sequence impedance angles on both sides of the fault are typically similar, the relationship between the zero-sequence currents on the M-side and N-side can be expressed as follows:

$$\begin{cases} \dot{I}_{MA} = I_{\text{mmc}}\angle\theta + \lambda\left|\dfrac{\dot{U}_{f1|0|}}{Z_{S1}+Z_{S2}+Z_{S0}+3R_f}\right|\angle-\theta_{AG} \\ \dot{I}_{NA} = (3-\lambda)\left|\dfrac{\dot{U}_{f1|0|}}{Z_{S1}+Z_{S2}+Z_{S0}+3R_f}\right|\angle-\theta_{AG} - I_{\text{mmc}}\angle\theta \end{cases} \quad (3)$$

During normal operation, the phase angle of the voltage remains nearly constant along the line. Therefore, $U_{f1|0}$ can be considered to be in phase with the reference phasor. The fault currents on both sides of the line are expressed as follows:

$$\begin{cases} \dot{I}_{MA} = I_{\text{mmc}}\angle\theta + \lambda\left|\dfrac{\dot{U}_{f1|0|}}{Z_{S1}+Z_{S2}+Z_{S0}+3R_f}\right|\angle-\theta_{AG} \\ \dot{I}_{NA} = (3-\lambda)\left|\dfrac{\dot{U}_{f1|0|}}{Z_{S1}+Z_{S2}+Z_{S0}+3R_f}\right|\angle-\theta_{AG} - I_{\text{mmc}}\angle\theta \end{cases} \quad (3)$$

Where $\boldsymbol{\theta_{AG}}$ denotes the equivalent impedance angle of the system. The fault currents on both sides are determined by the positive-sequence current from the MMC station and the zero-sequence current generated by the fault. Given the low-resistance grounding configuration, the zero-sequence current generally remains within the system's rated current, while the MMC's positive-sequence current remains close to the rated value. Consequently, the current amplitudes at both ends of the line during a single-phase ground fault are similar. However, under high transition resistance faults, it is possible that $|\boldsymbol{I_{MA}}| > |\boldsymbol{I_{NA}}|$.

When a phase-to-phase short-circuit fault (BC) occurs, no zero-sequence network is formed. Similar to the analysis of a single-phase earth fault, The analysis for three-phase short-circuits and two-phase grounding faults is similar to that described above and is not repeated here.

In summary, the following conclusions are drawn:

(1) Under severe faults on the tie line connected to the MMC station, the positive-sequence current from the MMC reaches its saturation limit, leading to a substantial difference in fault current magnitude between the MMC side and the grid side.

(2) For slight faults, the positive-sequence current from the MMC remains below the saturation limit. In this case, both the magnitude and phase angle of the MMC-side fault current depend on multiple factors such as fault type, power setpoint, and transition resistance. As a result, the current amplitudes on both sides of the faulted line may exhibit only minor differences.

III. Adaptability analysis of CDP

The CDP with a braking factor (K) is given as

$$\left|\dot{I}_{\text{m}} + \dot{I}_{\text{n}}\right| > K\left|\dot{I}_{\text{m}} - \dot{I}_{\text{n}}\right| \quad (4)$$

During an internal fault, the phase angle difference between the currents on both sides of the line is small. The differential current significantly exceeds the braking current, enabling accurate fault identification. In the case of an external fault, the fault currents on both sides of the line are approximately phase-opposed. As a result, the

differential current remains considerably smaller than the braking current, preventing the protection from operating.

It is evident that the phase angle θ of $\boldsymbol{I}_{mmc}$ is actively controlled. Consequently, the phase difference between the fault currents at both ends of the line varies with the operating condition of the MMC system, which adversely affects the performance of current differential protection (CDP). Furthermore, an earth fault introduces an uncontrolled zero-sequence current, complicating the phase relationship between the currents on the two sides. Therefore, the adaptability analysis of the CDP is conducted according to whether zero-sequence current is generated by the fault.

A. Single phase-to- ground fault

When a phase-A-to-ground fault occurs, the fault currents on both sides of the line —denoted as $\boldsymbol{I}_{MA}$ and $\boldsymbol{I}_{NA}$ —are determined by the positive-sequence current from the MMC and the zero-sequence current generated by the fault. Given that the system employs low-resistance grounding and assuming the MMC station operates under rated conditions, the positive-sequence current from the MMC side generally exceeds the zero-sequence current in magnitude. Its phase angle $\boldsymbol{\theta}$ can vary within the range (-π, 0). If the magnitude of the positive-sequence current remains constant during phase variations, the relationship between the fault current phasors at both ends of the line can be illustrated as shown in Fig. 4.

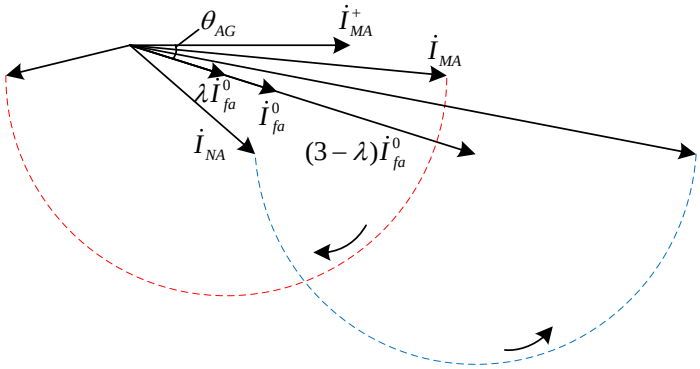

Figure 3 Vector graphic of A-phase current.

As $\boldsymbol{\theta}$ varies from 0 to -π, the endpoints of the current phasors $\boldsymbol{I}_{MA}$ and $\boldsymbol{I}_{NA}$ trace the paths indicated by the red and blue dashed curves, respectively. The vectors located at both ends of each curve correspond to the values at $\boldsymbol{\theta}$= 0 and $\boldsymbol{\theta}$ = -π. The arrows adjacent to the curves indicate the direction of movement as $\boldsymbol{\theta}$ decreases from 0 to -π.

As illustrated in Fig.3, as $\boldsymbol{\theta}$ decreases continuously, the phase difference $\Delta\boldsymbol{\theta}_{A}$ between the fault currents on the two sides of the line initially decreases from an acute angle to zero, then increases gradually to an obtuse angle. Furthermore, an increase in transition resistance reduces the zero-sequence current, which in turn expands the range of $\boldsymbol{\theta}$ values for which $\Delta\theta_a$ is obtuse. This effect can diminish the sensitivity of the differential protection and may eventually lead to its failure to operate.

B. Phase-to- phase fault

When the transition resistance is small, the fault current ($\boldsymbol{I}_{MB}$ *and* $\boldsymbol{I}_{MC}$) on the MMC side reaches its limit, and the amplitude of $\boldsymbol{I}_{NB}$ is significantly greater than $\boldsymbol{I}_{MB}$, as is the C phase. The relationship between the fault current vectors at both ends of the line is shown in figure 4 and 5.

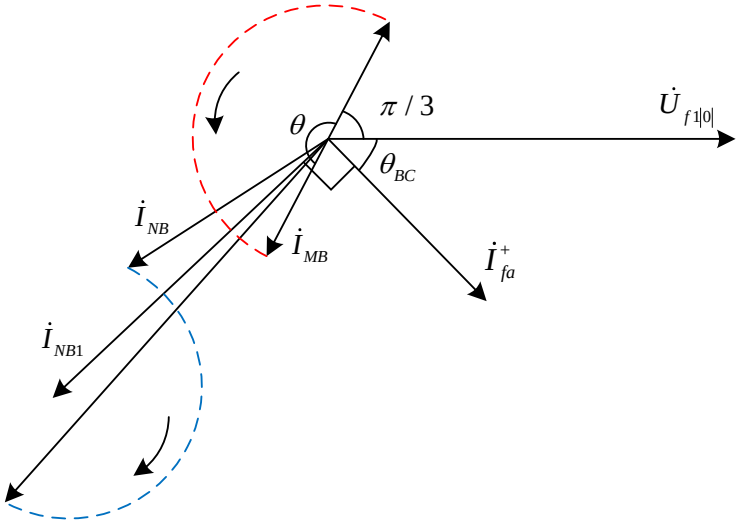

Figure 4 Vector graphic of B-phase current.

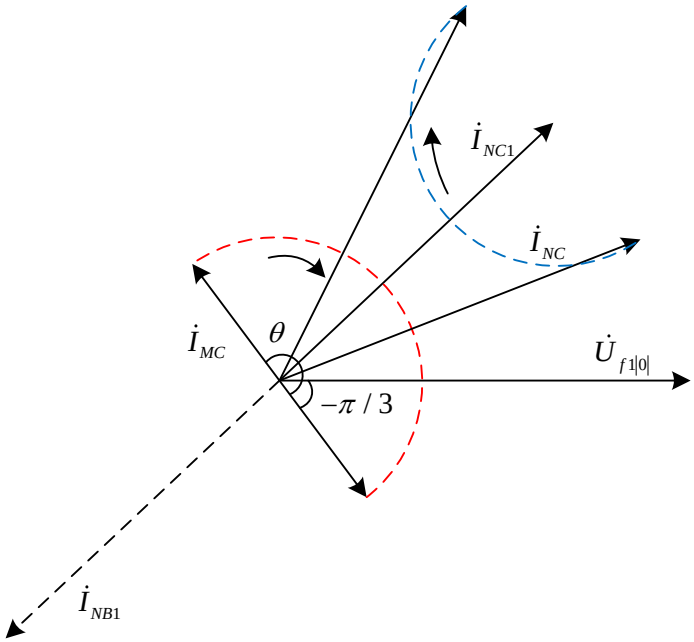

Figure 5 Vector graphic of C-phase current.

As $\boldsymbol{\theta}$ varies from 0 to -π, the phase difference $\Delta\boldsymbol{\theta_B}$ transitions from an acute angle to zero, then gradually increases to an obtuse angle. Simultaneously, the phase difference between $\boldsymbol{I_{MC}}$ and $\boldsymbol{I_{NC}}$ decreases from an obtuse angle to zero, before increasing again to an obtuse angle. Consequently, the CDP may maloperate, as both phase B and phase C can exhibit obtuse phase differences.The phase relationship between the fault currents on both ends of the line under high transition resistance is illustrated in Fig. 6.

The analysis of three-phase short circuits and two-phase grounding faults follows a similar logic. In summary, the primary reason for the poor performance of CDP on the AC-side tie line of an MMC station is that the phase difference between the fault currents at both ends of the line varies with the operating state of the MMC. This can result in an obtuse phase angle difference, which reduces the differential current while increasing the restraining current. As a consequence, the sensitivity of the CDP is diminished, and may even lead to protection failure. This issue is particularly pronounced in high-resistance faults, where the probability of an obtuse phase difference is higher, further reducing the reliability of the CDP.

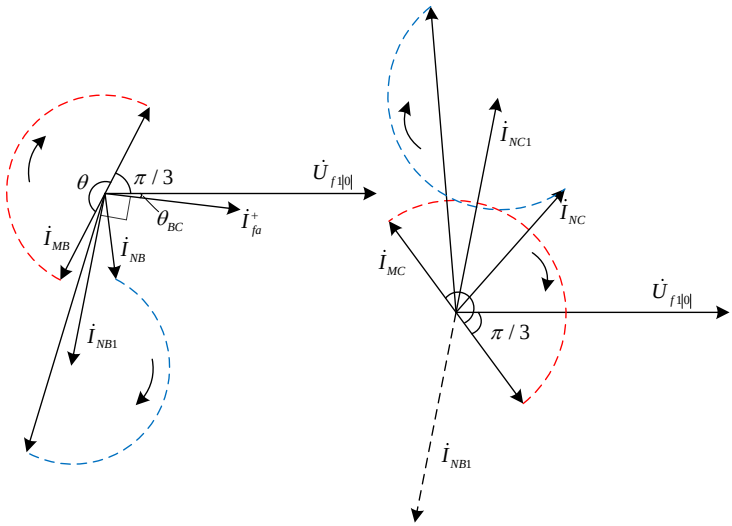

Figure 6 The phase relationship for a phase-to-phase high impedance fault.

IV. Improved CDP

The MMC's control strategy not only influences the phase of the fault current but also restricts its amplitude. Consequently, for most line faults, the amplitude difference between the fault currents at both ends remains significant. To enhance reliability, a new protection criterion is proposed that uses only the amplitude difference while disregarding phase relationships. The current amplitude differential protection criterion is given as:

$$\begin{cases} \left| \left| \dot{I}_{\max} \right| - \left| \dot{I}_{\min} \right| \right| > K \dfrac{\left| \dot{I}_{\max} \right| + \left| \dot{I}_{\min} \right|}{2} \\ \dot{I}_{\max} = \max\left\{ \dot{I}_{\mathrm{m}}, \dot{I}_{n} \right\}, \dot{I}_{\min} = \min\left\{ \dot{I}_{\mathrm{m}}, \dot{I}_{n} \right\} \end{cases} \quad (5)$$

Where the braking factor K is used to prevent the protection from operating incorrectly due to various factors. Equation (5) can be rewritten as:

$$\mu = \frac{\left| \dot{I}_{\min} \right|}{\left| \dot{I}_{\max} \right|} < \frac{2-K}{2+K} = \mu_{\mathrm{set}} < 1 \quad (6)$$

The reliable operation of current differential protection (CDP) relies on a substantial difference in fault current amplitude between the two ends of the line. While this allows correct operation under low transition resistance faults, the protection may fail to operate in high-resistance fault scenarios, where the MMC-side fault current remains below its limiting threshold.

Due to the control strategy of the MMC, the negative-sequence current differs significantly between the two ends of the faulty line, whereas the zero-sequence current shows only a minor difference. This distinct behavior of the negative-sequence current can be incorporated into the protection scheme to enhance fault identification and improve reliability.

For internal three-phase short-circuit faults, a clear amplitude difference exists between the two ends of the line. External faults, on the other hand, exhibit similar current amplitudes on both sides and can be easily identified using amplitude-based criteria. Therefore, the new protection principle should be designed such that the negative-sequence current characteristic is activated only during internal asymmetrical faults, without affecting the protection performance under other fault types.The new criterion is given as.

$$\mu = K_1 \frac{\left|\dot{I}_{\min}\right|}{\left|\dot{I}_{\max}\right|} < \frac{2-K}{2+K} = \mu_{set}, K_1 = \frac{\left|I_m^-\right| + k_2}{\left|I_n^-\right| + k_2} \quad (7)$$

Where $\boldsymbol{K_1}$ is the negative sequence current difference factor. I_m^- and I_n^- represent the negative sequence current amplitude on the MMC side and the grid side respectively. $\boldsymbol{k_2}$ is the negative sequence current action factor. $\boldsymbol{K_1}$ is only effective in the case of internal asymmetrical faults, thus avoiding any adverse effects on the amplitude differential protection caused by the introduction of the negative sequence characteristic. The $\boldsymbol{k_2}$ and the braking coefficient ($\boldsymbol{K}$) should be set according to CT transmission errors, synchronization errors, negative sequence unbalance current for external faults, etc.

V. Simulation and Discuss

A simulation model is constructed as shown in Fig 1 using MATLAB/Simulink, where f_2 is the midpoint of the line MN. The control mode of the MMC stations are mentioned in section 2. In the model, the rated DC voltage is ±10kV. The rated capacity of the MMC is 8MW. The voltage of the AC system is 10kV. The transformer turns ratio is 10kV/10kV, and its wiring form is Ynd11. Low-resistance grounding is adopted with an earthing resistance of 5Ω. The HJ line is a cable line. The lengths of HM, MN, and NJ are 3km, 4km, and 2km respectively. The positive sequence and zero sequence impedances of the line are 0.024+j0.162Ω/km and 0.196+j0.125Ω/km respectively. The protection sampling frequency is 10KHz.

A. Fault Characteristics of the Tie Line

To verify the above analysis, a phase-A to ground fault with different transition resistances occurs at the point *f*1 in Fig 1. The amplitude of each sequence current at points M and N during the fault is shown in Fig 7.

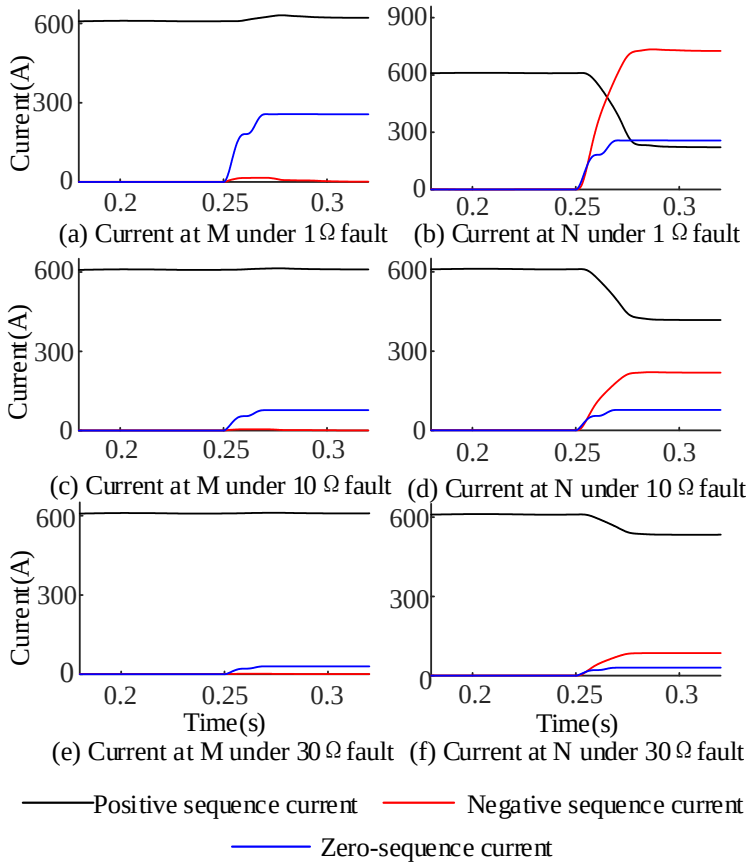

Figure 7 Current sequence components at M and N under different transition resistances.

The results of the operation characteristic for the CDP and the new protection are shown in Table 1 and Table 2 respectively. As the transition resistance increases, the CDP exhibits reduced sensitivity or even refuses to operate..

Table 1 Conventional CDP

Transition resistance /Ω	Operating current /A	Braking current /A	Sensitivity
1	1540	312	4.94
5	760	432	1.76
10	464	572	Failure to operate
20	261	706	Failure to operate
30	181	752	Failure to operate

However, as shown in Table 2 that $\mu<\mu_{set}$ always holds, indicating that the new protection scheme can act accurately.

Table 2 Improved CDP

Transition resistance /Ω	Protection criterion results(μ)	Action threshold(μ_{set})
1	0.012	0.45
5	0.015	0.45
10	0.022	0.45
20	0.034	0.45
30	0.063	0.45

B. Action characteristics for improved CDP

To verify the performance of the improved protection criterion proposed in this paper, the action characteristics of the protection under different types of faults are analyzed. Under different operating conditions of the MMC station, the operating characteristics of the new protection under different types of faults are shown in Fig 9.

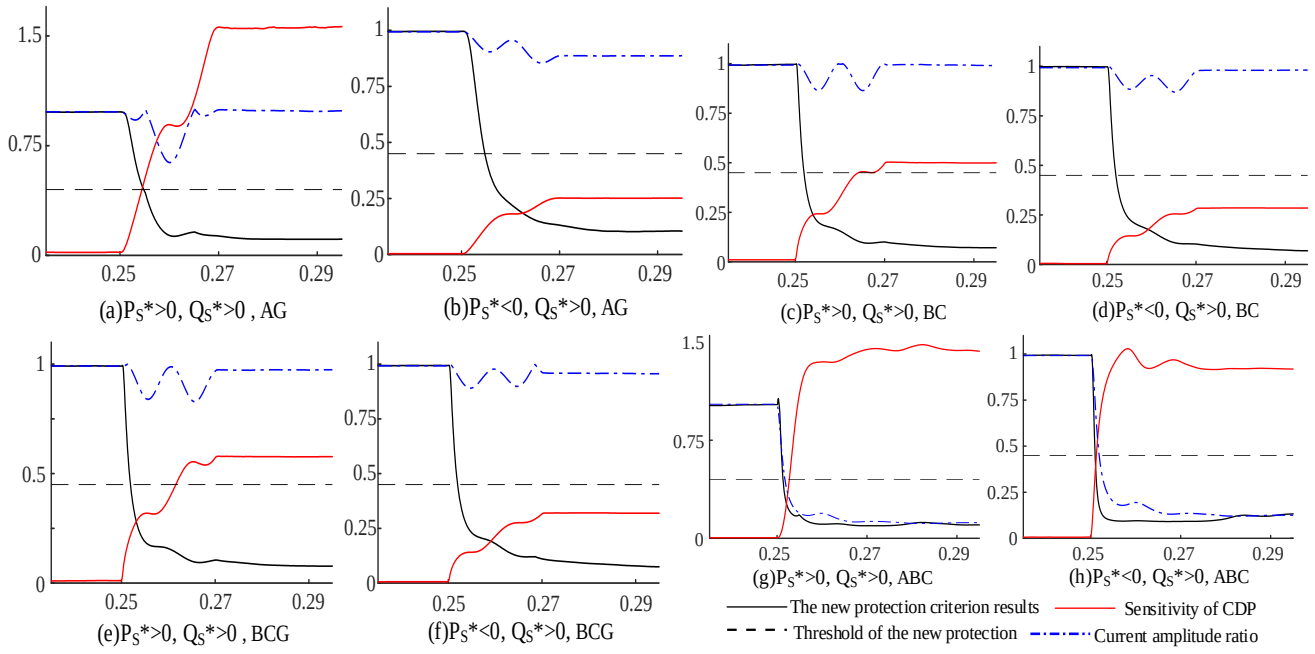

Figure 8 Protection performance under different faults.

As shown in Fig. 8, the improved protection scheme is largely unaffected by the operating status of the converter station. It accurately identifies faults even when current amplitudes on both sides of the faulted line are similar. Three-phase short

circuits are readily identified due to the significant current amplitude difference across the line. The performance of the new protection criteria under the aforementioned faults is summarized in Table 3. The results confirm that protections on adjacent lines (such as HM and NJ) remain secure and do not operate incorrectly for faults inside section MN, since the currents flowing through these external lines are through-currents. Both the fundamental and negative-sequence current differences remain small in such cases, ensuring that the proposed protection does not operate during external faults.

Table 3 The results of new protection criteria for external faults

Protection location	Operation states of the MMC station	AG	BC	BCG	ABC
Line HM	P_S*>0, Q_S*>0	0.986	0.993	0.991	0.996
	P_S*<0, Q_S*>0	0.994	0.994	0.994	0.995
Line NJ	P_S*>0, Q_S*>0	0.981	0.989	0.986	0.997
	P_S*<0, Q_S*>0	0.995	0.984	0.984	0.996

The reliability of the proposed protection scheme depends critically on the difference in negative-sequence current between both ends of the line, which is highly influenced by the fault transition resistance. Using a phase-A-to-ground fault as an example, the tolerance of the new criterion to transition resistance is evaluated at values of 10Ω, 20Ω, 30Ω, 50Ω, 80Ω and 100Ω.

Table 4 results under different resistances

Transition resistance/Ω	Amplitude ratio	Protection criterion results (μ)	Action threshold(μ_{set})
10	0.31	0.02	0.45
20	0.34	0.03	0.45
30	0.51	0.06	0.45
50	0.65	0.12	0.45
80	0.79	0.20	0.45
100	0.83	0.24	0.45

As shown in Table 4, as the transition resistance increases, the difference in current amplitude ratio between the two ends of the line gradually decreases, suggesting that the transition resistance tolerance of conventional current amplitude differential protection is limited. However, beyond fault current amplitude difference, the new scheme also incorporates the negative-sequence current amplitude difference at both ends to enhance fault characteristics, ensuring that $\boldsymbol{\mu<\mu_{set}}$ continues to hold. Thus, the proposed scheme ensures reliable operation even under high-impedance fault conditions.

VI. Conclusion

This paper first investigates the fault characteristics of the AC-side tie line in the MMC station and analyzes how the fault current varies with the MMC control strategy. A improved CDP method is then proposed to address the limitations of conventional CDP.

(1) Under commonly used MMC control strategies, the negative-sequence current on the MMC side is effectively suppressed to near zero, while the positive-sequence current amplitude is also limited. This results in a significant difference in current amplitude between the two ends of the faulty line.

(2) The amplitude and phase of the MMC-side current exhibit wide variations under controller regulation, reducing the reliability of traditional CDP. During internal faults, the phase relationship between currents on both sides becomes uncertain, and in extreme cases, the phase difference may become obtuse. This leads to a decrease in differential current, an increase in restraining current, and a higher risk of protection failure.

(3) The proposed method enhances fault identification during internal faults by utilizing the negative-sequence current characteristics and the amplitude difference between currents at both line ends. It exhibits higher tolerance to transition resistance, is less influenced by the operating state

of the MMC station, and demonstrates improved sensitivity and reliability compared to conventional CDP. Additionally, the method reduces the dependency on communication conditions.

References

1. X. Dong et al., "Morphological characteristics and technology prospect of new distribution system," High Voltage Engineering, vol.47, no.9, pp. 3021-3035, Sep. 2021.
2. Sanghita & C. Nandi., "A comprehensive review on DC Microgrid protection schemes," Electr. Power Syst. Res., 210 (2022): 108051.
3. Chandra, G K. Singh, V. Pant., "Protection techniques for DC microgrid-A review. " Electr. Power Syst. Res., 187 (2020): 106439.
4. L. Zhang et al., "Converting AC distribution lines to DC to increase transfer capacities and DG penetration," IEEE Trans. Smart Grid., vol.10, no.2, pp.1477-1487, 2018.
5. Ali. Zulfiqar et al., "Fault management in dc microgrids: A review of challenges, countermeasures, and future research trends," IEEE Access, vol.9, pp.128032-128054, Sep. 2021.
6. X. Li, L. Guo, D. Huang, Y. Zhao & C. Wang, "Research Review on Operation and Control of DC Distribution Networks," High Voltage Engineering, vol.45, no.10, pp.3039-3049, Oct. 2019.
7. Elsayed, A. Mohamed, & O. Mohammed. "DC microgrids and distribution systems: An overview," Electr. Power Syst. Res., 119 (2015): 407-417.
8. Kumar, F. Zare &A. Ghosh, "DC microgrid technology: system architectures, AC grid interfaces, grounding schemes, power quality, communication networks, applications, and standardizations aspects," IEEE Access, vol.5, pp.12230-12256, 2017.
9. S. Jiang et al., "Current situation and prospect of demonstration projects of DC distribution system," Electric Power Automation Equipment, vol.41, no.5, pp. 219-231, May. 2021.
10. Z. Wang, J. Su, Y. Cui, T. Wei & W. Zhang, "Research on the structures and application scenarios of medium voltage AC-DC hybrid distribution network," in 2019 IEEE 3rd Information Technology, Networking, Electronic and Automation Control Conference (ITNEC), Mar. 2019, pp.743-747.
11. S. Xue, J. Yang, Y. Chen, C. Wang, Z. Shi, M. Cui, & B. Li, "The applicability of traditional protection methods to lines emanating from VSC-HVDC interconnectors and a novel protection principle," Energies, vol.9, no.6, pp.400-427, May. 2016.
12. Xiao, W. Han, Q. Li, & X. Xiong, "Adaptability of MMC-HVDC System on Relay Protection of AC Transmission Lines," Smart Power, vol.48, no.04, pp.1-8, Jan.2020.
13. Y. Gao et al., "Short-Circuit Current Calculation Method For AC/DC Power Transmission Systems With MMC," Acta Energiae Solaris Sinica, vol.43, no.8, pp.17, Aug. 2022.
14. G. Bu, Y. Li, S. Wang, B. Zhao, T. Wang & Y. Yang, "Analysis of the Short-circuit Current of MMC-HVDC," Proceedings of the CSEE, vol.37, no.21, pp.6303-6312, Nov. 2017.
15. Y. Liang, W. Li, Z. Lu, F. Zhao & W. Zha, "Influence of MMC-HVDC on current phase differential protection of AC line," Electric power automation equipment, vol.39, no.9, pp.95-101, Sep.2019.
16. B. Shi, G. Sun, R. Jin, J. Xie & Y. Wang, "Influence Study of VSC-HVDC Interconnection on AC Line Differential Protection," in 2019 IEEE 8th International Conference on Advanced Power System Automation and Protection (APAP), Oct 2019, pp. 1340-1345.
17. Y. Li, B. Shi, J. Xie, G. Sun, Y. Wang, & M. Jin, "Influence study of Chongqing-Hubei VSC-HVDC interconnection on 500 kV AC line differential protection," Power System Protection and Control, vol.47, no.20, pp.149-155, Oct. 2019.
18. B. Li et al., "Improved Differential-current protection For AC Transmission Line Connecting Renewable Energy Power Plant And MMC-HVDC System," in 2021 IEEE Sustainable Power and Energy Conference (ISPEC), Dec 2021, pp.787-791.
19. Y. Liang, Y. Ren & W. He, "An Enhanced Current Differential Protection for AC Transmission Lines Connecting MMC-HVDC Stations," IEEE Systems Journal, vol.17, no.1, pp.892-903, Mar. 2023.
20. Y. Liang, & Z. Lu, "Adaptive Differential Protection Principle Based on Compensation Coefficient for Active Distribution Network,"

Power System Technology, vol.46, no.6, pp.2268-2275, Nov. 2022.
21. L. Zheng, K. Jia, T. Bi, Y. Fang & Z. Yang, "Cosine similarity based line protection for large-scale wind farms," IEEE Trans. Ind. Electron., vol.68, no.7, pp.5990-5999, Jul. 2020.
22. Y. Gao, Y. Li, X. Chen, Z. Zhao, Q. Wang & J. Ren, "Adaptive Differential Protection Principle for Active Distribution Network Based on Current Amplitude Ratio," Proceedings of the CSU-EPSA, vol.33, no.2, pp.1-7, Feb. 2021.
23. Casagrande et al., "A differential sequence component protection scheme for microgrids with inverter-based distributed generators," IEEE Trans. Smart Grid., vol. 5, no. 1, pp. 29-37, Jan. 2014,
24. H. Gao, L. Juan, and B. Xu., "Principle and implementation of current differential protection in distribution networks with high penetration of DGs," IEEE Trans. Power Deliv., vol. 32, no. 1, pp. 565-574, Feb. 2017
25. S. Chen, N. Tai, C. Fan, J. Liu & S. Hong, "Sequence-component-based current differential protection for transmission lines connected with IIGs," IET Renew. Power Gener., vol.12, no.12, pp.3086-3096, Apr. 2018.
26. J. Yang, Y. Liu, W. Su, X. Xiao, X. Si & X. Zhang, "Grounding fault on DC side of Suzhou Tongli ±10 kV flexible DC distribution system," Electric Power Engineering Technology, vol.40, no.6, pp.113-120, Nov. 2021.